Colloids and Surfaces B: Biointerfaces 150 (2017) 106–113

Contents lists available at ScienceDirect

Colloids and Surfaces B: Biointerfaces

journal homepage: www.elsevier.com/locate/colsurfb

Membrane effects of dihydropyrimidine analogues with larvicidal activity

Mariela E. Sánchez-Borzone[a,1], Maria E. Mariani[a,1], Virginia Miguel[a,1], Raquel M. Gleiser[b], Bharti Odhav[c], Katharigatta N. Venugopala[c], Daniel A. García[a,*]

[a] Instituto de Investigaciones Biológicas y Tecnológicas (IIByT-CONICET), Cátedra de Química Biológica, Facultad de Ciencias Exactas, Físicas y Naturales, Universidad Nacional de Córdoba, Córdoba, Argentina
[b] Centro de Relevamiento y Evaluación de Recursos Agrícolas y Naturales (CREAN), Instituto Multidisciplinario de Biología Vegetal (IMBIV), CONICET, Universidad Nacional de Córdoba, Córdoba, Argentina
[c] Department of Biotechnology and Food Technology, Durban University of Technology, Durban, South Africa

ARTICLE INFO

Article history:
Received 15 June 2016
Received in revised form
18 November 2016
Accepted 22 November 2016
Available online 24 November 2016

Keywords:
Dihydropyrimidine
Larvicidal
Membrane interaction
Monolayers
Membrane fluidity
Molecular dynamic simulations

ABSTRACT

Two recently synthesized dihydropyrimidines (DHPMs) analogues have demonstrated larvicide and repellent activity against *Anopheles arabiensis*. DHPMs high lipophilicity suggests that these compounds may interact directly with the membrane and modify their biophysical properties. The purpose of the present study was to characterize the interaction of both compounds with artificial membranes. Changes on the properties of DPPC films were studied using Langmuir monolayers. The presence of DHPMs in the subphase modified the interfacial characteristics of DPPC compression isotherms, causing the expansion of the monolayer, inducing the disappearance of DPPC phase transition and increasing the molecular packing of the film. Moreover, both compounds showed ability to penetrate into the lipid monolayers at molecular pressures comparable to those in biological membranes. The effects of both DHPMs on the molecular organization of DPPC liposomes were measured by fluorescence anisotropy. The results indicate that their presence between lipid molecules would induce an increasing intermolecular interaction, diminishing the bilayer fluidity mainly at the polar region. Finally, we performed free diffusion MD simulations and obtained spatially resolved free energy profiles of DHPMs partition into a DPPC bilayer through Potential of Mean Force (PMF) calculations. In agreement with the experimental assays, PMF profiles and MD simulations showed that DHPMs are able to partition into DPPC bilayers, penetrating into the membrane and stablishing hydrogen bonds with the carbonyl moiety. Our results suggest that DHPMs bioactivity could involve their interaction with the lipid molecules that modulate the supramolecular organization of the biological membranes and consequently the membrane proteins functionality.

1. Introduction

The pyrimidine system is an important pharmacophore with abundant occurrence in nature. Natural and synthetic pyrimidine derivatives have a wide range of actions with biological activities such as anticancer, by altering the mitotic spindle and arresting mitosis [1], as well as antiviral [2,3], antihypertensive [4], calcium channel blocking [5], antitubercular [6], antimicrobial [7–9], anti-inflammatory [10,11], larvicidal and insecticide actions [12,13]. Antimalarial drugs include halogenated dihydropyrimidine analogues [14] and the commercially available pyrimethamine, a folic acid antagonist used for treatment and prevention of malaria or, with a sulfonamide, to treat toxoplasmosis [15].

Dihydropyrimidines (DHPMs) are useful scaffolds for the design of pharmacological agents. Despite the fact that the exact mechanisms responsible for their biological activity remain unknown, disturbance of the cell membrane has been suggested as the mode of actions of several larvicide compounds [16]. The wide range of effects produced by DHPMs and their high lipophilicity suggest that these compounds may interact directly with the membrane and thus activate different signals.

Previous studies have shown that the interaction of lipophilic compounds with the membrane can be explained by an equilibrium model of partition [17] and that their partition into the membrane

* Corresponding author at: Instituto de Investigaciones Biológicas y Tecnológicas (IIBYT), CONICET, Universidad Nacional de Córdoba, Av. Vélez Sarsfield, 1611, Córdoba, 5016, Argentina.
E-mail addresses: dagarcia@unc.edu.ar, dasmedgarcia@yahoo.com (D.A. García).
[1] First co-authors- these authors contributed equally to this work.

http://dx.doi.org/10.1016/j.colsurfb.2016.11.028
0927-7765/

modifies its biophysical properties. This behavior has been confirmed for lipophilic compounds such as benzodiazepines (BZD), whose location in the polar region of the membrane explains their effects, decreasing the size of DPPC vesicles, inducing lipid bilayer redistribution and inhibiting inverted phases formation, which are crucial intermediaries in fundamental biological phenomena such as membrane fusion [18–20]. The possibility that BZDs affect transduction mechanisms at several levels of receptor binding has also been shown for other lipophilic substances [21,22].

Many experimental evidences show that changes in the cell membrane microenvironment, where intrinsic proteins as specific receptors and channels are inserted, can modify their function [23–27]. Such is the case described by our group, where several gabaergic compounds (i.e. monoterpenes and phenols) that modulate the $GABA_A$ receptor allosteric behavior, also are capable of modifying membrane properties [28–32].

In the present work, we investigated the ability of two recently synthesized DHPMs with insecticidal activity (Fig. 1) [13], to interact with the membrane by analyzing their effects on the biophysical properties of two artificial model membranes: i) Langmuir monolayers at the air-water interface, where compression and penetration isotherms were analyzed, and ii) phospholipid liposomes yielded to fluorescence anisotropy analysis. Furthermore, we combined these experimental techniques with molecular dynamics (MD) simulations of DHPMs partition into the bilayer.

2. Materials and methods

2.1. Materials

2-(3-Bromophenylamino)-6-(4-chlorophenyl)-5-(methoxycarbonyl)-4-methyl-3,6-dihydropyrimidin-1-ium chloride (DHPM1) and 2-(4-bromophenylamino)-6-(4-chlorophenyl)-5-(methoxycarbonyl)-4-methyl-3,6-dihydropyrimidin-1-ium chloride (DHPM6) were synthesized according to Venugopala et al., 2013 [13]. DPH and TMA-DPH (*N,N,N*-trimethyl-4-(6-phenyl-1,3,5-hexatrien-1-yl)phenylammonium*p*-toluenesulfonate) were obtained from Sigma-Aldrich Chem (St. Louis, MO; USA) and l-2-dipalmitoyl-sn-glycero-3-phospocholine (DPPC) lipid were purchased from Avanti Polar Lipids (Alabaster, AL, USA). All other reagents were of the highest analytical grade. Solutions were prepared with double-deionized water.

2.2. Langmuir monolayers

2.2.1. Surface pressure (π) – molecular area (A) isotherms

Compression isotherms (π/A isotherms) were performed by the compression of monolayers containing DPPC using a Minitrough II (KSV, Finland). Phospholipidic monolayers on the air–water interface were prepared by spreading pure DPPC dissolved in chloroform on the aqueous surface of a Teflon™ trough filled with bidistilled-deionised water containing each DHPM at a final concentration of 100 μM as subphase. After 5 min for solvent evaporation, the film was compressed isometrically at a constant rate of 5 ± 1 mm/min until reaching the target pressure. Lateral surface pressure (π) was measured with a platinum plate by the Wilhelmy plate method [33] at different molecular areas (A) of the phospholipid. Isotherms were averaged at least from duplicates. All assays were performed at 25 ± 1 °C.

2.2.2. Compressibility analysis

The onset of phase transition points was identified from a minimum and π_c from a maximum in the variation of the *compressibility modulus* (*K*) vs. molecular area plot. For this, *K* values were calculated from π-A isotherms data applying Eq. (1):

$$K = -(A_\pi)\left(\frac{\delta_\pi}{\delta_A}\right)\pi \quad (1)$$

where Aπ is the molecular area at the indicated surface pressure. Control isotherms obtained in the presence of DMSO 0.25% (v/v) (used as DHPMs dissolvent) were not different from those at 0% DMSO (data not shown).

2.2.3. Penetration isotherms: partition into lipid interface

To study the penetration of the DHPMs into DPPC lipid monolayers, π *vs.* time plots in a Langmuir trough at constant total surface area were performed, using double deionized water as subphase.

Penetration experiments were carried out in circular home-made Teflon through by injections of DHPMs, from stock solutions in DMSO, into the subphase (100 μM final concentrations) under continuous stirring (150–250 rpm) at different initial π (π_i), in order to measure the increment in π induced by the penetration into a preformed DPPC monolayer as a function of time. The injection of each DHPM in the sub-phase was done after the stabilization of the π_i of the film (between 5 and 10 min) at 25 ± 1 °C. Initially, π vs. time plots were measured until an equilibrium surface pressure was reached (changes in pressure less than 1 mN m^{-1} per hour). Finally, plots of $\Delta\pi$ vs. π_i were graphed in order to determine the "*cut off*" point for both DHPMs.

2.3. Fluorescence anisotropy

2.3.1. Preparation of large unilamellar vesicles

Multilamellar large vesicles (MLVs) were prepared as described elsewhere [34]. Briefly, the appropriate amount of DPPC dissolved in chloroform was placed in a glass tube and evaporated under a stream of nitrogen with constant rotation to facilitate the formation of a thin lipid film; traces of solvent were removed under vacuum. The dried lipid was suspended in water at a final concentration of 0.03 mg/mL [35] by repeating seven consecutive cycles of heating at 65 °C for 1 min plus vortexing for 30 s, and MLVs were formed. Large unilamellar vesicles (LUVs) of homogeneous size were obtained by extruding 19 times the MLVs suspension trough 100-nm pore size Whatman polycarbonate filters using a miniextruder Liposofast (Avestin, Canada).

2.3.2. Steady-State fluorescence

The fluorescent probes DPH (4 μM) and TMA-DPH (6 μM) were added to the DPPC-LUV suspension (prepared as described above) and incubated for 1 h at room temperature [36]. The effect of DHPMs (100 μM) on DPH and TMA-DPH steady-state fluorescence anisotropy was studied. Anisotropy values were calculated from the emission fluorescence intensities at $\lambda_{em} = 430$ nm ($\lambda_{ex} = 356$ nm) measured with the excitation and the sample polarizer filters oriented parallel and perpendicularly one with respect to the other, in a L-format FluoroMax-3 spectrofluorometer (JovinYvon, Horiba, Japan). Slits width and integration time were set at 2 nm and 1 s, respectively. Control samples containing DMSO used as vehicle were tested to rule out the effect of this solvent.

Steady-state fluorescence anisotropy (FA) was calculated using Eq. (2):

$$FA = \frac{I_{VV} - I_{VH}.G}{I_{VV} + 2I_{VH}.G}, G = \frac{I_{HV}}{I_{HH}} \quad (2)$$

where I_{VV}, I_{HH}, I_{VH}, and I_{HV} are the values of the different measurements of fluorescence intensity taken with both polarizers in vertical (VV) and horizontal (HH) orientations or with the excitation polarizer vertical and the emission polarizer horizontal (VH) or

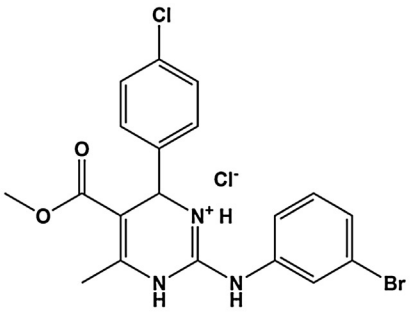

2-(3-Bromophenylamino)-6-(4-chlorophenyl)-5 -(methoxycarbonyl)-4-methyl- 3,6-dihydropyrimidin-1-ium chloride (**DHPM 1**)

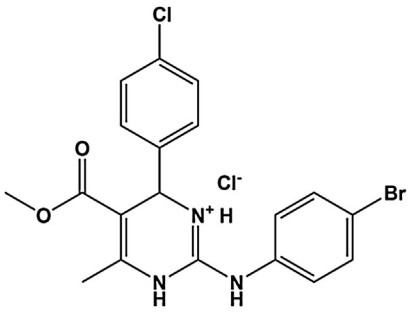

2-(4-Bromophenylamino)-6-(4-chlorophenyl)-5- (methoxycarbonyl)-4-methyl- 3,6-dihydropyrimidin-1-ium chloride (**DHPM 6**)

Fig. 1. Chemical structure and IUPAC names of the test compounds.

vice versa (HV). G is a correction factor for differences in sensitivity of the detection system for vertically and horizontally polarized light [34].

2.4. Computational details

All simulations were carried out using the 4.6.3 Gromacs package with GPU acceleration [37]. The All Atom (AA) Slipids was used for lipids [38] and the TIP3P model [39] for water molecules. The starting geometries were obtained from Slipids on line resource (http://mmkluster.fos.su.se/slipids/).

The construction of DHPM units to be used in MD simulations was obtained with the antechamber module, using the GAFF force field, [40] as described before [41]. The Ante Chamber PYthon Parser interfacE (ACPYPE) [42] was employed to change the format of the parameter files in order to use them with Gromacs code. Gaussian 03 package [43] was used for DHPMs quantum chemical calculation.

The Potential of Mean Force (PMF) simulations were carried out in a fully hydrated lipid DPPC bilayer containing 64 molecules, equilibrated at 50 °C. Free energy profile calculations were derived from the PMF $\Delta G(z)$ calculation as a function of the distance of the DHPMs to the bilayer center along the z-axis normal to the plane of the bilayer. A series of 20 separate simulations, of 10 ns each, were performed, in which each molecule was restrained to a given depth in the bilayer by a harmonic restraint on the z-coordinate. A force constant of 1000 kJ mol^{-1} nm^{-2} was used with a spacing of 0.2 nm between the centers of the biasing potentials. Two DHPM molecules were used, one per leaflet allowing error estimation. Finally, the Weighted Histogram Analysis Method (WHAM) was used to extract the PMF and calculate $\Delta\Delta G$ [44]. The error bars for these calculations were obtained using the bootstrap method [45]. For long-range, neighbour cut-off value was set at 1.6 nm.

Fully hydrated lipid bilayers equilibrated at 50 °C and containing 128 DPPC molecules were employed for equilibrium MD simulations. For free diffusion MD, the simulation protocols were the same detailed before [38,41]. Five DHPMs molecules were located at random starting positions within 5 to 25 Å over the membrane plane. We used the MD parameters available in the Stockholm lipids home page (http://mmkluster.fos.su.se/slipids/). All bonds were constraint using Lincs algorithm. Constraining the bond lengths allowed a time step of 2 fs to be used. The Lennard-Jones interactions were truncated at 1.0 nm. The particle mesh Ewald method [46] was used to evaluate the electrostatic interactions, with a cut-off of 1.0 nm. The simulations were performed at an NPT ensemble. ~200 ns of MD simulations at 50 °C within the NPT ensemble were collected for all the systems, and the final 100 ns of these simulations were employed for analysis.

3. Results and discussion

The interaction between surface active compounds and phospholipids has been extensively studied in several model membrane systems [47,48]. In the present study, we evaluate the membrane interaction of two larvicidal DHPMs (called DHPM1 and DHPM6 according to Venugopala et al., 2014 [13]) by analyzing their effects on the molecular properties of phospholipidic monomolecular films and liposomes, and by MD simulations of their partition into the bilayer.

3.1. Compression isotherms and effects of rheological properties

The Langmuir films assays were performed by using DPPC lipid monolayers which are ideal for understanding lipid-compounds interactions. Phospholipid monolayers constitute simple models to study intermolecular interactions [49–51] since the interface can be easily modulated by changing interfacial composition or lateral packing [52,53].

In presence of DHPMs in the subphase, the isotherms presented an expansion of liquid expanded phases (LE) (Fig. 2A), suggesting that they would act as spacers between DPPC molecules. The value of the minimal molecular area (MMA) (corresponding to the collapse pressure) found in the present work for pure DPPC monolayers is in agreement with other reports (~40 Å/molecule) [54]. Since both DHPMs increased the MMA of DPPC, and considering that the MMA corresponds to the area required for the phosphorylcholine group, its expansion in the presence of DHPMs suggest that the insertion of the compounds between the host phospholipid molecules would occur near the polar head group level. It is worth mentioning that the position of the Br atom on the aminophenyl ring is the only structural difference among both DHPM molecules. Given that DHPM6 caused the highest effect on MMA expansion, it is expected that the bromine atom at position 4 of the phenylamine ring induces a more defined dipole moment, considering the relatively closer position of Br respect to the Cl atoms. In this sense, the value of dipole moment calculated for DHPM6 (~0.2 mD), effectively duplicates the value obtained for DHPM1. Taking into account that this parameter affects the hydrophobic-hydrophilic balance of the molecule, it is expected that differences observed on monolayer expansion are due to the differences in the contribution of both DHPM on dipole moment of the polar region of lipid molecules [55]. Other consequences of this structural difference among both DHPM will be discussed again in accordance with the computational analysis (see below).

Monolayers may exist in different phase states depending on the temperature or surface pressure. Different phase states involve different degrees of freedom or molecular order due to the inter-

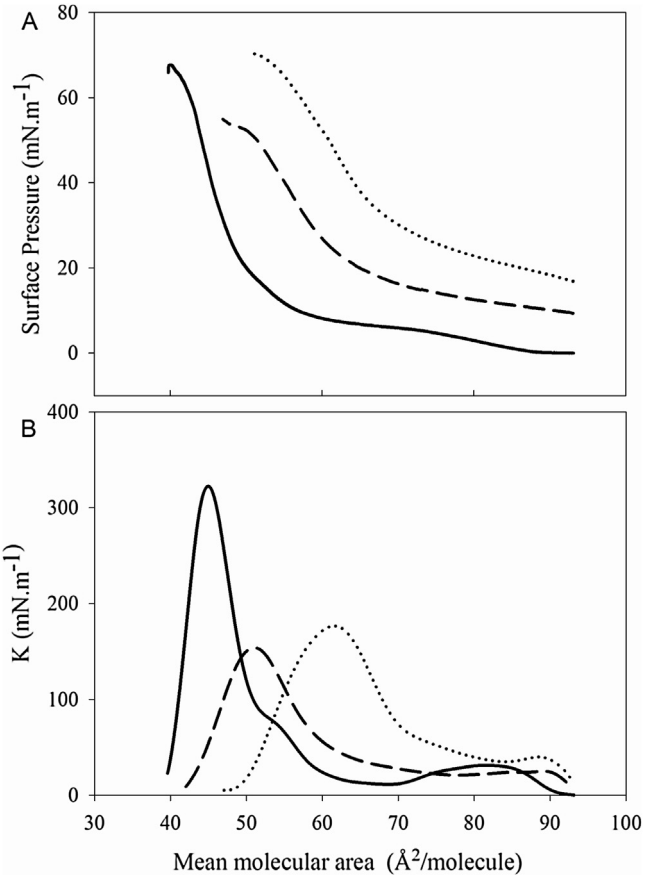

Fig. 2. Effect of molecular compression on the interfacial properties of DPPC Langmuir films. **(A)** Compression isotherms.**(B)** K (*compressibility modulus*) values, calculated from π-A curves according to Eq. (1), vs. mean molecular area. Curves were obtained in the absence (control solid line) or in the presence of DHPMs (100 μM): DHPM1 (long dash) and DHPM6 (dotted line). Assays were performed at 25 ± 1 °C.

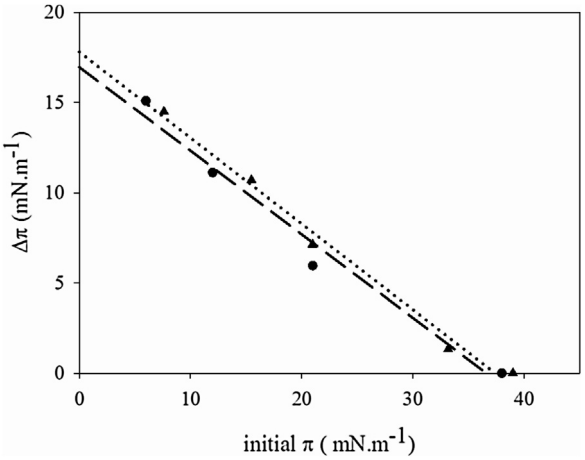

Fig. 3. Penetration of DHPMs in DPPC monomolecular films (Δπ vs. initial π). The DHPMs were assayed at a final concentration of 100 μM in the subphase at different initial surface pressures between 6 and 40 mN m^{-1} for DHPM1 (long dash-filled circles) and DHPM6 (dotted line-filled triangles).

molecular forces present in and between the film and the subphase [56]. The compressibility modulus (K), calculated from the π-A compression isotherms, reflects variations in the physical state of the films and it is frequently determined to study the monolayer phase behavior. The maximum compressibility modulus value obtained in the present work for DHPM1 (153.86 mN m^{-1}) was slightly smaller than the displayed in the presence of DHPM6 (189.11 mN m^{-1}), being both values quite lower than that observed for pure DPPC (322.45 mN m^{-1}) (Fig. 2B). In liquid condensed phases (LC), where the molecules are arranged with the greatest possible packing, a high modulus means that the film responds to compression with a large increase in pressure. Conversely, in LE phases, where molecules that form the film have lower molecular interaction, lower K values are interpreted as moderated progressive packing as the molecular area decreases. The presence of the DHPMs in the subphase changed the shape of the π-A isotherm and decreased the K values, indicating a higher film elasticity. Moreover, both DHPMs allowed the occurrence of the compressibility modulus main peak at larger molecular areas respect to pure DPPC, indicating their ability to induce a relatively larger increment in the molecular packing of the film. In this context, DHPM6 showed a major effect respect to DHPM1, in agreement with the greater expansion shown before.

The π-Area isotherm of DPPC monolayer in absence of DHPMs showed the characteristic transition phase from LE to LC state (Fig. 2A, solid line). The presence of both DHPMs apparently caused the loss of a clear phase transition in the isotherms. However, the analysis of the compressibility modulus plots indicates that the transition occurs at higher molecular areas according to a small peak present with both DHPM assayed (Fig. 2B).

3.2. Penetration profile of DHPMs in monomolecular films

To characterize the ability of the DHPMs to penetrate and insert into phospholipid monolayers, DHPMs were added to the subphase of a preformed monomolecular film of DPPC at different initial π values (π_i). An increase in π_i was observed in the plots of π vs. time (data not shown), suggesting a clear interaction of the lipophilic compounds with the membrane of DPPC.

The *"cut off"* parameter represents the maximum pressure at which a lipophilic compound is capable of inserting into the monolayer and is related to more or less favorable interaction of the drug with the membrane. As observed in Δπ vs. π_i plots in Fig. 3, the incorporation of DHPMs into the monolayer was favored by less-packed film structures. Both compounds showed *cut off* values close to 37 mN.m^{-1}. Thus, partition of DHPM into bilayers is expected, considering that the average lateral pressure in natural membranes is around 35 mN m^{-1} [30].

3.3. Anisotropy analysis

Anisotropy values for DPH and TMA–DPH in DPPC LUVs were evaluated as a function of temperature (36–46 °C) in the presence of DHPM1 or DHPM6 (100 μM) (Fig. 4). Fluorescence anisotropy gives information about the organization of the membrane environment around the fluorescent probe. DPH is known to be located within the hydrocarbon chain region of the membrane core, while TMA–DPH, due to its polar ionic portion, is located near the interfacial region in the polar head group region [57]. The complex structural dynamics of the bilayers is governed by temperature-dependent parameters such as the average interfacial area per lipid, thickness of bilayer, and disorder of hydrophobic tails, which determine their phase behavior. For saturated phosphatidylcholines, such as DPPC, the main transition between the liquid-crystalline phase and the gel phase (gel–fluid transition) occurs at 41.5 °C [58,59].

The temperature dependences of DPH and TMA–DPH fluorescence anisotropy on control samples containing DPPC (without any compound) showed an abrupt change at approximately 41.5 °C in agreement with the phase transition of DPPC [58] (Fig. 4A and B solid line). Both compounds decreased the membrane fluidity at

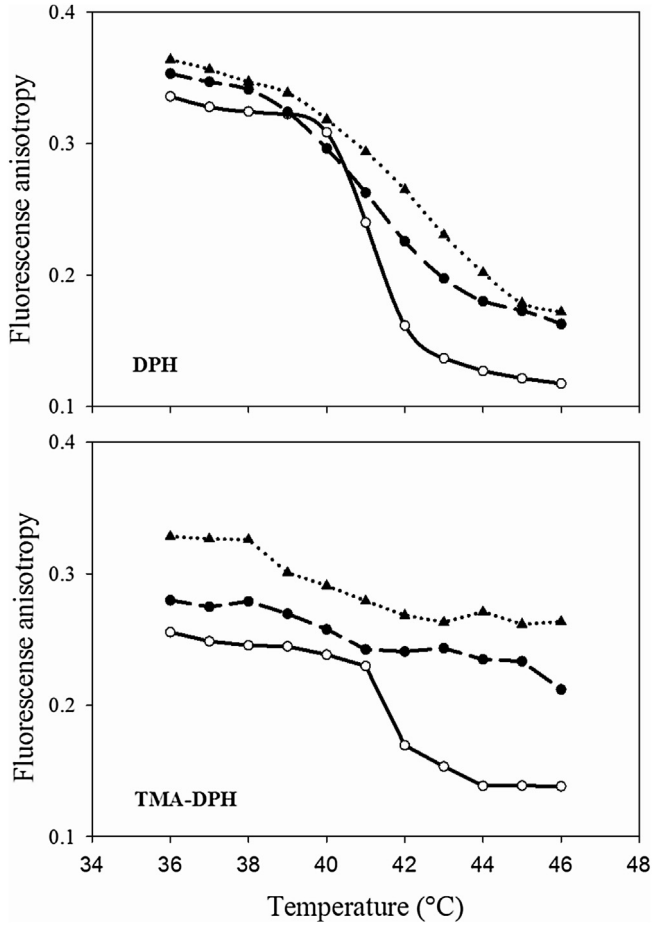

Fig. 4. Effects of DHPMs on temperature dependence of DPH and TMA–DPH fluorescence anisotropy in DPPC LUVs. Control (solid line-empty circles), DHPM1 (long dash-filled circles) and DHPM6 (dotted line-filled triangles).

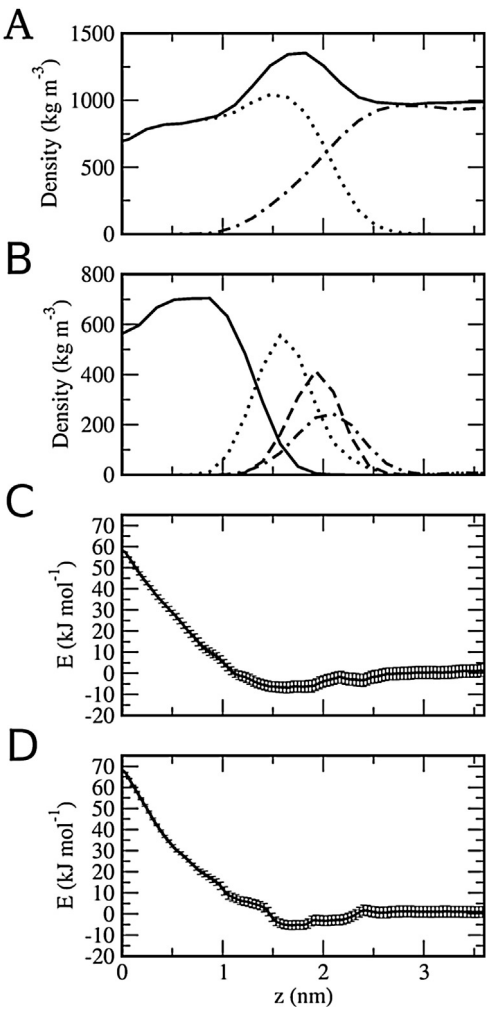

Fig. 5. Free energy (ΔG) of partitioning into a DPPC bilayer. The partial densities of the different chemical groups of the system are shown. **(A)** System (solid line), Water (dash-dotted line) and DPPC (dotted line). **(B)** Choline (dash-dotted line); phosphate (dashed line); carbonyls (dotted line); hydrocarbon chain (solid line). Free energy (*ΔG*) PMF of partition for **(C)** DHPM1 and **(D)** DHPM6 in a DPPC bilayer at liquid-crystalline phase (50 °C). Error bars were obtained by bootstrap analysis using g_wham.

different depths and at different membrane phase states (Fig. 4A and B dash and dotted lines), being this effect more noticeable with TMA-DPH probe (Fig. 4B). This effect indicates that the presence of DHPMs between lipid molecules induces an enhancement of the intermolecular interaction, increasing the molecular order throughout the bilayer thickness, but mainly at the polar interface region, confirming their partition into the bilayer, but away from the hydrocarbon chains region. The decreased fluidity induced by both DHPMs on DPPC bilayers is in correspondence with the observed for monolayers, where at a determined molecular area, they induced a more packed film.

3.4. Molecular dynamics simulation of DHPMs

We present MD simulation studies of the interaction of DHPMs with a model bilayer of DPPC. Free energy calculations were used to describe the partition process of DHPMs into the bilayer. PMF calculations were performed to determine the probable distribution of these two compounds at different places of the lipidic system.

Spatially resolved free energy profiles of DHPMs partition into a DPPC bilayer in the liquid-crystalline phase were obtained through PMF calculations using an umbrella sampling technique as a function of the distance to the center of the bilayer along its normal axis z [ΔG(z)]. All MD simulations were performed for DPPC at 50 °C (Fig. 5). PMF curves were aligned so that the relative free energy in bulk water corresponds to zero in each case. The molecular ratio DHPM:DPPC is 1:32.

The shape of the free energy profiles was similar for both compounds. The global energy minimum is approx. −7 kJ mol^{-1} within the carbonyl region of DPPC (1.5 nm) (Fig. 5), while the maximum is in the center of the bilayer (0 nm). The ΔG value for transferring a DHPM molecule from water to the bilayer center was 60 kJ mol^{-1}, approximately. According to the results obtained with PMF calculations, the most favored location of DHPMs is within the carbonyl region of DPPC, which correspond to the interphase between the hydrophobic and the polar zone of the bilayer, being less favored their placement between the hydrocarbon chains. These results also indicate that both compounds are able to partition into a DPPC bilayer, penetrating to the polar head region. Due to the presence of a large energy barrier in the middle of the bilayer, DHPMs crossing the barrier is expected to be a rare event. PMF results are in agreement with those observed in the anisotropy and lipid monolayer assays, indicating that DHPMs interact with the membrane preferentially at the polar region.

We performed free diffusion MD simulations to gain insight into the specific interactions of each compound with the bilayer. Fully hydrated lipid bilayers equilibrated at 50 °C, containing 128 DPPC molecules and five DHPMs molecules were run for 200 ns. To corroborate the proper equilibration of the simulations, the

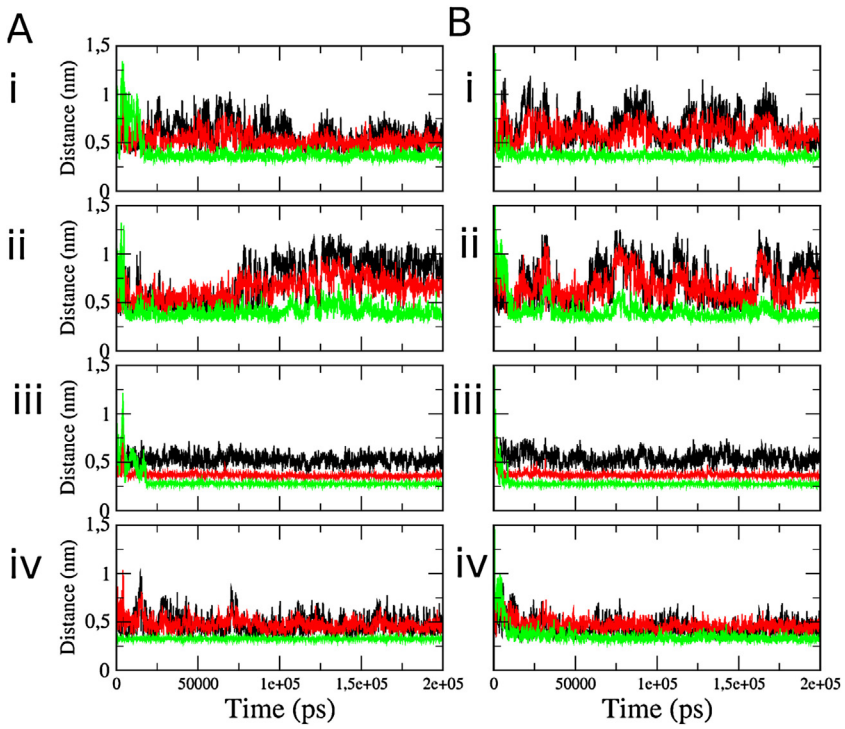

Fig. 6. Minimum distance among atoms or groups from **(A)** DHPM1 or**(B)** DHPM6 and different groups of DPPC molecules. The lines represent the minimum distance among **i-**Br, **ii-**Cl, **iii**-Amine group and **iv**-O from DHPM molecule, and choline (black line), phosphate (red line) and carbonyl (green line) groups from DPPC molecule. (For interpretation of the references to colour in this figure legend, the reader is referred to the web version of this article.).

area per lipid (APL) and membrane thickness were evaluated (data not shown). The density profile during the last 100 ns simulation along the normal to the membrane plane (z-axis) of different DPPC membrane components and DHPMs molecules, was calculated (Fig. S1). The peak of DHPMs density in the membrane was found in the region of the carbonyl groups of DPPCs indicating that DHPM molecules are preferentially located in this region. This profile is consistent with the free energy profile obtained from the PMF (Fig. 5).

The degree of ordering of the acyl chains of the phospholipids can be determined from the deuterium order parameter (DOP), S_{CD} [60]. This parameter was employed to evaluate the effect of the interaction of DHPMs with the membrane in the order of the acyl chains (Fig. S2). Although the increase in S_{CD} values was mild, the presence of DHPMs molecules induced a more order state in hydrocarbonate chains. No differential effect among the two DHPMs was observed.

We analyzed the chemical groups that interact when DHPM enters the bilayer following the variation of the minimum distance among these groups (Fig. 6). This analysis showed that both DHPM amine groups interact with DPPC carbonyl and in less extend with phosphate groups. The main difference observed between DHPM1 and DHPM6 is the distance among their Br and Cl atoms with the DPPC headgroup (choline and phosphate). The Br atom of DHPM1 is located in close contact with the polar head while the Cl is placed at larger distance that is nearer to the hydrophobic region. In the other hand, the distance values to the phospholipid polar head for both atoms (Cl and Br) of DHPM6 were more fluctuant, indicating a less restrained movement of this compound. We also analyzed the hydrogen bonds between DHPMs molecules with DPPC. An average of two hydrogen bonds per DHPM molecule was presented for both DHPMs (Fig. S3). DHPM amine moieties formed hydrogen bonds with oxygens from the carbonyl group of DPPC, and with oxygens from the phosphate group (data not shown).

Theoretical models and experimental results confirm that both DHPM molecules are interacting mainly with the phospholipid carbonyl region through their central part (amine moieties). The differential behavior of their opposite ends, Cl and Br atoms, explains the relatively larger effects experimentally demonstrated for DHPM6 on the bilayer order and monolayer expansion. A more fluctuant placement of these atoms between both phospholipid regions (see above) would induce not only a major structural restraining (higher order) but also an increment in the apparent volume of polar region (higher expansion). Furthermore, the ability to establish hydrogen bonds is in agreement with the stabilization of DHPMs in the carbonyl region of bilayer. This location in the named “interfacial” zone of the phospholipid molecule, restraining its resonance forms, would justify the ordering effect of both compounds not only in the polar headgroup region of the bilayer but also in the fatty acyl chains [61].

4. Conclusions

We showed that the DHPMs studied are lipophilic compounds that modify the lipid monolayers by their incorporation into the film up to molecular pressures comparable to those expected for natural membranes, increasing its molecular packing.

The effect of both DHPMs on the molecular organization of liposomes indicates that their presence between lipid molecules induces an increasing intermolecular interaction, diminishing the bilayer fluidity mainly at the polar region.

MD simulations showed an energetically favorable partition of DHPM molecules to the membrane, principally at the carbonyl region of the bilayer, in accordance with the experimental results presented in this work, probably due to hydrogen bonds between the phospholipid carbonyl region and the DHPM amine moieties.

Thus, we conclude that DHPMs are clearly able to interact with membranes, and provide insight into the mechanism of molecular interactions between DHPMs and membrane phospholipids.

Taking into account their capability to change the physical properties of the lipid bilayer, it is possible to consider that the DHPM interaction with the lipid molecules, modulating the supramolecular organization of biological membranes and consequently the membrane proteins functionality, contributes at least in part as an action mechanism which explains the DHPMs bioactivity.

Conflict of interest

The authors declare no conflicts of interest.

Acknowledgements

The authors are grateful to SECyT-Universidad Nacional de Córdoba, FONCyT, CONICET (PIP 2011 and 2014) (Argentina), National Research Foundation (South Africa) (Grant number 91995) and Durban University of Technology, for support and facilities. MSB, VM, RMG, and DAG are CONICET Career Members. MEM is a postdoctoral fellow from CONICET. This work is a result of a bilateral collaboration between MinCyT – Argentina and NRF – South Africa.

Appendix A. Supplementary data

Supplementary data associated with this article can be found, in the online version, at http://dx.doi.org/10.1016/j.colsurfb.2016.11.028.

References

[1] T.U. Mayer, T.M. Kapoor, S.J. Haggarty, R.W. King, S.L. Schreiber, T.J. Mitchison, Small molecule inhibitor of mitotic spindle bipolarity identified in a phenotype-based screen, Science 29 (1999) 5441.
[2] E.W. Hurst, R. Hull, Two new synthetic substances active against viruses of the psittacosis-lymphogranuloma-trachoma group, J. Med. Pharm. Chem. 3 (1961) 215–229.
[3] X. Zhu, G. Zhao, X. Zhou, X. Xu, G. Xia, Z. Zheng, L. Wang, X. Yang, S. Li, 2,4-Diaryl-4,6,7,8-tetrahydroquinazolin-5(1H)-one derivatives as anti-HBV agents targeting at capsid assembly, Bioorg. Med. Chem. Lett. 20 (2010) 299–301.
[4] S.A. Karnail, N.S. Brian, E.U. Steven, M.F. David, M. Suzanne, H. Anders, C.O.R. Brian, Dihydropyrimidine calcium channel blockers. 3. 3-Carbamoyl-4-aryl-1,2,3,4-tetrahydro-6-methyl-5-pyrimidinecarboxylic acid esters as orally effective antihypertensive agents, J. Med. Chem. 34 (1991) 806–811.
[5] B. Jauk, T. Pernat, C.O. Kappe, Design and synthesis of a conformationally rigid mimic of the dihydropyrimidine calcium channel modulator SQ 32,926, Molecules 5 (2000) 227–239.
[6] K.N. Venugopala, S.K. Nayak, M. Pillay, P. Renuka, Y. Coovadia, B. Mohamed, Synthesis Odhav anti-tubercular activity of 2-(substituted phenyl/benzyl-amino)-6-(4-chlorophenyl)-5-(methoxycarbonyl)-4-methyl-3, 6-dihydropyrimidin-1-ium chlorides, Chem. Biol. Drug Des. 81 (2013) 219–227.
[7] A.E.S. Wael, F.N. Ibrahim, A.H. Adel, R. Abdel, C-Furyl glycosides, II: synthesis and antimicrobial evaluation of C-furyl glycosides bearing pyrazolines, isoxazolines, and 5 6-dihydropyrimidine-2(*1H*)-thiones, Monatsh. Chem. 140 (2009) 365–370.
[8] T.B. Shah, A. Gupte, M.R. Patel, V.S. Chaudhari, H. Patel, V.C. Patel, Synthesis and in vitro study of biological activity of heterocyclic N-Mannich bases of 3, 4-dihydropyrimidine-2(1H)-thiones, Indian J. Chem. 49B (2010) 578–586.
[9] R.J. Nevagi, A.S. Dhake, H.I. Narkhede, P. Kaur, Design, synthesis and biological evaluation of novel thiosemicarbazide analogues as potent anticonvulsant agents, Bioorg. Chem. 54 (2014) 68–72.
[10] S.B. Sushilkumar, B.S. Devanand, Synthesis and anti-inflammatory activity of some 2-amino-6-(4-substituted aryl)-4-(4-substituted phenyl)-1,6-dihydropyrimidine-5-yl-acetic acid derivatives, Acta Pharm. 53 (2003) 223–229.
[11] Z.M. Nofal, H.H. Fahmy, E.S. Zarea, W. El-Eraky, Synthesis of new pyrimidine derivatives with evaluation of their anti-inflammatory and analgesic activities, Acta Pol. Pharm. 68 (2011) 507–517.
[12] E. Rajanarendar, M.N. Reddy, K.R. Murthy, K.G. Reddy, S. Raju, M. Srinivas, B. Praveen, M.S. Rao, Synthesis, antimicrobial, and mosquito larvicidal activity of 1-aryl-4-methyl-3 6-bis-(5-methylisoxazol-3-yl)-2-thioxo-2,3,6,10b-tetrahydro-1H-pyrimido[5,4-c]quinolin-5-ones, Bioorg. Med. Chem. Lett. 20 (2010) 6052–6055.
[13] K.N. Venugopala, R.M. Gleiser, R.K. Chalannavar, B. Odhav, Antimosquito properties of 2-substituted phenyl/benzylamino-6-(4-chlorophenyl)-5-methoxycarbonyl-4-methyl-3,6-dihydropyrim idin–ium chlorides against Anopheles arabiensis, Med. Chem. 10 (2014) 211–219.
[14] E.L. Stogryn, Effect of trifluoromethoxy, chlorodifluoromethoxy, and trifluoromethyl on the antimalarial activity of 5-benzyl- and 5-phenyl-2 4-diaminopyrimidines, J. Med. Chem. 16 (1973) 1399–1401.
[15] M.N.S. Saudi, M.R. Gaafar, M.Z. El-Azzouni, M.A. Ibrahim, M.M. Eissa, Synthesis and evaluation of some pyrimidine analogs against toxoplasmosis, Med. Chem. Res. 17 (2008) 541–563.
[16] A. Ghosh, N. Chowdhury, G. Chandra, Plant extracts as potential mosquito larvicides, Indian J. Med. Res. 135 (2012) 581.
[17] M.A. Perillo, A. Arce, Determination of the membrane-buffer partition coefficient of flunitrazepam, a lipophilic drug, J. Neurosci. Methods 36 (1991) 203–208.
[18] D. García, M. Perillo, Supramolecular events modulate flunitrazepam partitioning into natural and model membranes, Colloids Surf.(B) 9 (1997) 49–57.
[19] D.A. Garcia, M.A. Perillo, Benzodiazepine localisation at the lipid-water interface: effect of membrane composition and drug chemical structure, Biochim. Biophys. Acta 1418 (1999) 221–231.
[20] D.A. Garcia, M.A. Perillo, Effects of flunitrazepam on the Lalpha-H(II) phase transition of phosphatidylethanolamine using merocyanine 540 as a fluorescent indicator, Colloids Surf. B Biointerfaces 37 (2004) 61–69.
[21] M.A. Perillo, A. Polo, A. Guidotti, E. Costa, B. Maggio, Molecular parameters of semisynthetic derivatives of gangliosides and sphingosine in monolayers at the air-water interface, Chem. Phys. Lipids 65 (1993) 225–238.
[22] J.M. Sonner, R.S. Cantor, Molecular mechanisms of drug action: an emerging view, Annu. Rev. Biophys. 42 (2013) 143–167.
[23] A. Guidotti, M.G. Corda, B.C. Wise, F. Vaccarino, E. Costa, GABAergic synapses. Supramolecular organization and biochemical regulation, Neuropharmacology 22 (1983) 1471–1479.
[24] M.R. Witt, M. Nielsen, Characterization of the influence of unsaturated free fatty acids on brain GABA/benzodiazepine receptor binding in vitro, J. Neurochem. 62 (1994) 1432–1439.
[25] M.R. Witt, M. Nielsen, Differential modulation of brain benzodiazepine receptor subtypes by ricinelaidic acid in vitro, Biochem. Pharmacol. 47 (1994) 742–744.
[26] M. Pytel, K. Mercik, J.W. Mozrzymas, Interaction between cyclodextrin and neuronal membrane results in modulation of GABA(A) receptor conformational transitions, Br. J. Pharmacol. 148 (2006) 413–422.
[27] R. Sogaard, T.M. Werge, C. Bertelsen, C. Lundbye, K.L. Madsen, C.H. Nielsen, J.A. Lundbaek, GABA(A) receptor function is regulated by lipid bilayer elasticity, Biochemistry 45 (2006) 13118–13129.
[28] N.A. Corvalan, J.A. Zygadlo, D.A. Garcia, Stereo-selective activity of menthol on GABA(A) receptor, Chirality 21 (2009) 525–530.
[29] M.A. Perillo, D.A. Garcia, R.H. Marin, J.A. Zygadlo, Tagetone modulates the coupling of flunitrazepam and GABA binding sites at $GABA_A$ receptor from chick brain membranes, Mol. Membr. Biol. 16 (1999) 189–194.
[30] M.E. Sanchez, A.V. Turina, D.A. Garcia, M.V. Nolan, M.A. Perillo, Surface activity of thymol: implications for an eventual pharmacological activity, Colloids Surf. B Biointerfaces 34 (2004) 77–86.
[31] D.A. Garcia, J. Bujons, C. Vale, C. Suñol, Allosteric positive interaction of thymol with the $GABA_A$ receptor in primary cultures of mouse cortical neurons, Neuropharmacology 50 (2006) 25–35.
[32] G. Reiner, L. Delgado-Marin, N. Olguin, S. Sanchez-Redondo, M. Sánchez-Borzone, E. Rodriguez-Farre, C. Suñol, D.A. Garcia, GABAergic pharmacological activity of propofol related compounds as possible enhancers of general anesthetics and interaction with membranes, Cell Biochem. Biophys. 67 (2013) 515–525.
[33] R. Verger, G.H. de Haas, Enzyme reactions in a membrane model 1: a new technique to study enzyme reactions in monolayers, Chem. Phys. Lipids 10 (1973) 127–136.
[34] A.D. Bangham, M.W. Hill, N.G.A. Miller, Preparation and use of liposomes as models of biological membranes, Methods Membr. Biol. (1974) 1–68.
[35] M.G. Gore, Spectrophotometry and Spectrofluorimetry: a Practical Approach, Oxford University Press, 2000.
[36] M.P. Zunino, A.V. Turina, J.A. Zygadlo, M.A. Perillo, Stereoselective effects of monoterpenes on the microviscosity and curvature of model membranes assessed by DPH steady-state fluorescence anisotropy and light scattering analysis, Chirality 23 (2011) 867–877.
[37] B. Hess, C. Kutzner, D. van der Spoel, E. Lindahl, GROMACS 4: algorithms for highly efficient, load-balanced, and scalable molecular simulation, J. Chem. Theory Comput. 4 (2008) 435–447.
[38] J.P. Jambeck, A.P. Lyubartsev, Derivation and systematic validation of a refined all-atom force field for phosphatidylcholine lipids, J. Phys. Chem. B 116 (2012) 3164–3179.
[39] W.L. Jorgensen, J. Chandrasekhar, J.D. Madura, R.W. Impey, M.L. Klein, Comparison of simple potential functions for simulating liquid water, J. Chem. Phys. 79 (1983) 926.
[40] J. Wang, R.M. Wolf, J.W. Caldwell, P.A. Kollman, D.A. Case, Development and testing of a general amber force field, J. Comput. Chem. 25 (2004) 1157–1174.
[41] V. Miguel, M.E. Defonsi Lestard, M.E. Tuttolomondo, S.B. Diaz, A.B. Altabef, M. Puiatti, A.B. Pierini, Molecular view of the interaction of S-methyl methanethiosulfonate with DPPC bilayer, Biochim. Biophys. Acta 1858 (2015) 38–46.
[42] A.W. Sousa da Silva, W.F. Vranken, ACPYPE—AnteChamber PYthon parser interfacE, BMC Res. Notes 5 (2012) 367.

[43] M. Frisch, G.W. Trucks, H. Schlegel, G.E. Scuseria, M.A. Robb, J.R. Cheeseman, J.A. Montgomery, T. Vreven, K.N. Kudin, J. Burant, Gaussian 03, revision C. 02, (2008).
[44] S. Kumar, J.M. Rosenberg, D. Bouzida, R.H. Swendsen, P.A. Kollman, THE weighted histogram analysis method for free-energy calculations on biomolecules. I. The method, J. Comput. Chem. 13 (1992) 1011–1021.
[45] J.S. Hub, B.L. de Groot, D. van der, Spoel, g_wham—a free weighted histogram analysis implementation including robust error and autocorrelation estimates, J. Chem. Theory Comput. 6 (2010) 3713–3720.
[46] U. Essmann, L. Perera, M.L. Berkowitz, T. Darden, H. Lee, L.G. Pedersen, A smooth particle mesh Ewald method, J. Chem. Phys. 103 (1995) 8577–8593.
[47] P. Dynarowicz-Latka, A. Dhanabalan, O.N. Oliveira Jr., Modern physicochemical research on Langmuir monolayers, Adv. Colloid Interface Sci. 91 (2001) 221–293.
[48] C. Peetla, A. Stine, V. Labhasetwar, Biophysical interactions with model lipid membranes: applications in drug discovery and drug delivery, Mol. Pharm. 6 (2009) 1264–1276.
[49] O. Albrecht, H. Gruler, E. Sackmann, Pressure-composition phase diagrams of cholesterol/lecithin, cholesterol/phosphatidic acid, and lecithin/phosphatidic acid mixed monolayers: a langmuir film balance study, J. Colloid Interface Sci. 79 (1981) 319–338.
[50] R.A. Demel, Monolayers–description of use and interaction, Methods Enzymol. 32 (1974) 539–544.
[51] H. Möhwald, Phospholipid Handbook, Editor; G. Cevec, (1993) 579–602.
[52] J. Imbenotte, M.C. Verger, High molecular weight rapidly labelled ribonucleic acid (RNA) and virus production in chick fibroblasts infected with avian myeloblastosis virus. Comptes rendus hebdomadaires des seances de l'Academie des sciences, Ser. D: Sci. Nat. 276 (1973) 1049–1052.
[53] B. Maggio, D. Raffa, M.V. Raimondi, M.G. Cusimano, F. Plescia, S. Cascioferro, G. Cancemi, M. Lauricella, D. Carlisi, G. Daidone, Synthesis and antiproliferative activity of new derivatives containing the polycyclic system 5,7:7,13-dimethanopyrazolo[3,4-b]pyrazolo[3',4':2,3]azepino[4,5-f]azocine, Eur. J. Med. Chem. 72 (2014) 1–9.
[54] B. Caruso, D.M. Maestri, M.A. Perillo, Phosphatidylcholine/vegetable oil pseudo-binary mixtures at the air-water interface: predictive formulation of oil blends with selected surface behavior, Colloids Surf. B Biointerfaces 75 (2010) 57–66.
[55] R. Maget-Dana, The monolayer technique: a potent tool for studying the interfacial properties of antimicrobial and membrane-lytic peptides and their interactions with lipid membranes, Biochim. Biophys. Acta 1462 (1999) 109–140.
[56] J.G.L. Gaines, Insoluble Monolayers at Liquid-Gas Interfaces, Wiley-Interscience, New York, 1966.
[57] F.G. Prendergast, R.P. Haugland, P.J. Callahan, 1-[4-(Trimethylamino)phenyl]-6-phenylhexa-1,3,5-triene: synthesis, fluorescence properties, and use as a fluorescence probe of lipid bilayers, Biochemistry 20 (1981) 7333–7338.
[58] R.L. Biltonen, D. Lichtenberg, The use of differential scanning calorimetry as a tool to characterize liposome preparations, Chem. Phys. Lipids 64 (1993) 129–142.
[59] Z.V. Leonenko, E. Finot, H. Ma, T.E.S. Dahms, D.T. Cramb, Investigation of temperature-induced phase transitions in DOPC and DPPC phospholipid bilayers using temperature-controlled scanning force microscopy, Biophys. J. 86 (2004) 3783–3793.
[60] A. Seelig, J. Seelig, The dynamic structure of fatty acyl chains in a phospholipid bilayer measured by deuterium magnetic resonance, Biochemistry 13 (1974) 4839–4845.
[61] C.H. Huang, A structural model for the cholesterol-phosphatidylcholine complexes in bilayer membranes, Lipids 12 (1977) 348–356.